

Rotokawa Conceptual Model Update 5 years After Commissioning of the 138 MWe NAP Plant

¹Sewell, S. M., ¹Addison, S.J., ¹Hernandez, D., ¹Azwar, L., ¹Barnes, M.L.

¹Mighty River Power Limited, 283 Vaughan Road, Rotorua 3010

Steven.Sewell@mightyriver.co.nz

Keywords: *Rotokawa, conceptual model, Nga Awa Purua*

ABSTRACT

This paper describes the development of the main conceptual model elements that have been used as a basis for numerical modelling and well targeting at the Rotokawa Geothermal Field. These elements are largely based on characterising the natural state of the reservoir, prior to production, but significant new knowledge has been gained from monitoring the response of the reservoir to the start of the 138 MWe Nga Awa Purua (NAP) plant in 2010. Characterising the natural state pressure, temperature and geochemistry of the system has been crucial to the conceptual model development, particularly the location of deep upflows and outflows. The lateral extent of the convecting permeable reservoir has been interpreted using a combination of natural state temperature and MT resistivity surveys. A significant confined aquifer called the “intermediate aquifer” exists above the reservoir and contains variably mixed geothermal fluids and groundwater in the Rotokawa area. Flows within this aquifer and between the deep reservoir and intermediate aquifer have been characterised based on natural state temperatures, alteration, MT surveys and geology and topography. Low permeability caps occur above both the deep reservoir and the intermediate aquifer, formed by smectite-altered formations that are identified in wells via conductive temperature profiles and methylene blue measurements, imaged by MT surveys as low resistivity zones. Major geologic structures have been identified within the field based on detailed analysis of stratigraphic offset between the wells and microseismic data. These structures appear to be controlling the compartmentalised response of the reservoir under production, which has been identified through pressure and geochemistry monitoring since the start of production. The depth of microseismicity has provided some indication of the effective base of the reservoir for numerical modelling, however this is unconfirmed by drilling. Hydrology of the shallow unconfined aquifer is based on the geochemistry of surface features, shallow monitoring well pressures, temperatures, chemistry and by surface geology and topography.

1. INTRODUCTION

The Rotokawa geothermal field is located within the Taupo Volcanic Zone (TVZ) a centre of active rifting in the North Island of New Zealand (Figure 1). The resource potential of the Rotokawa field was first identified from numerous surface thermal features, including acid sulphate fumaroles, steaming ground and bi-carbonate springs, and from resistivity surveys (Schlumberger soundings). Exploratory drilling undertaken from 1965 to 1986 by the New Zealand government (RK1 – RK6, RK8) confirmed the presence of a large, high temperature ($>300^{\circ}\text{C}$) geothermal resource. Early geology (e.g. Grindley et al., 1985; Browne, 1989), geochemistry (e.g. Hedenquist et al., 1988) and reservoir engineering (e.g. Grant, 1985) based on data from these wells was used to form an early understanding of the

hydrology within the field that is largely consistent with the current understanding. A recent review paper by McNamara et al., (2015) summarises most of the historical geoscience work on the Rotokawa field.

Electricity generation of 24 MWe began on the field in 1997 with the installation of the Rotokawa (RKA) binary plant. Production was initially from wells RK5 and RK9 with shallow injection at about 500 to 1000 m depth into RK1, RK11, and RK12. In 2000, Mighty River Power and Tauhara North No. 2 Trust formed the Rotokawa Joint Venture and generation was subsequently expanded to 34 MWe. Following analyses of well results and 1D/2D MT-TDEM resistivity imaging, shallow injection was shifted to deeper zones at ~1000-3000m depth in RK16 and RK18 in 2005.

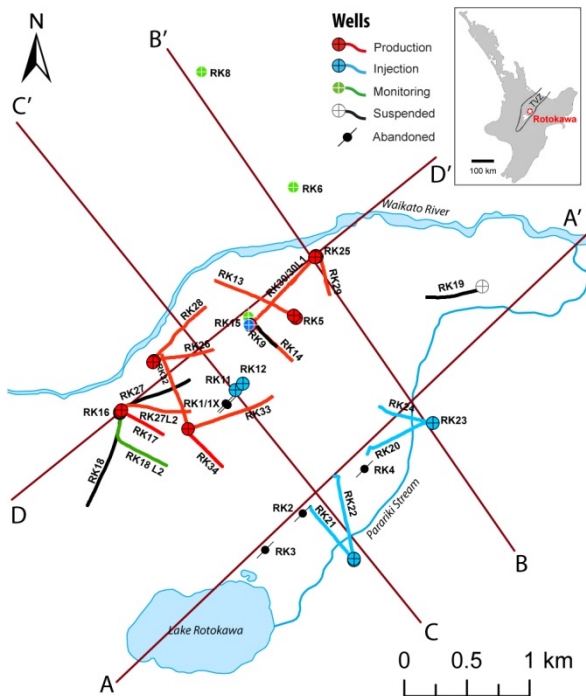


Figure 1: Production, injection, monitoring and suspended wells at the Rotokawa Geothermal Field as of 2015. The inset shows the location of the field on the North Island of New Zealand. The location of cross-sections in Figures 2, 5 & 6 are also shown.

In 2007, resource consents were obtained for a further development at Rotokawa, supported by conceptual and numerical modelling of the field based on production history (RKA plant) and well results up to RK18 (Bowyer & Holt, 2010). The Nga Awa Purua (NAP) development

began in 2008 with the drilling of wells RK19 to RK30 and construction of a 138 MWe, triple-flash plant which was commissioned in early 2010. Since then make-up production wells RK32, RK33 and RK34 have been drilled.

Following NAP start-up in 2010, the conceptual and numerical models of the field were revised. Significantly more information had been obtained since the last update in 2007, most importantly the information obtained from drilling of wells RK19 – RK33 and the initial response of the Rotokawa reservoir to greatly increased production and injection. Hernandez et al., (2015a), and Addison et al., (2015a), provide reviews of the thermodynamic and chemistry responses of the reservoir since NAP start-up respectively. This paper describes the main elements of the conceptual model that were developed mainly in 2010-2011, but has since been updated with new information obtained from production and injection since 2011. The conceptual model described here is considered the most likely model that best fits the currently available data.

2. CONCEPTUAL MODEL ELEMENTS

The main goal of developing the conceptual model was to provide the framework for development of a numerical model of the geothermal system that would subsequently be used as the main tool for reservoir management. Given this, the conceptual model was divided into a number of elements with each element representing an important input into the numerical model (Hernandez et al., 2015b). Dividing the conceptual model in this way, and constructing cross-sections and maps showing the location of the different elements, was an effective way of providing input to numerical modellers (Figure 2). The following describes the conceptual elements and the data that supports the interpretation of these elements.

2.1 Deep Upflows and Outflows

The natural state temperature of the reservoir, based on interpretation of temperature logs after drilling, shows the highest measured temperatures occur in the southern part of the reservoir (Figure 3). The maximum measured temperature is 337 °C in RK22, currently the highest measured temperature of the drilled geothermal fields in New Zealand. Natural state reservoir temperatures show cooling towards the northwest with temperatures ~20 °C cooler in the northern-most production wells (~310 °C in RK13 and RK28). A strong lateral gradient in natural state reservoir chemistry also occurs from southeast to northwest (Figure 3). Based on natural state reservoir temperature and chemistry, there are two main models proposed for the deep natural flows within the geothermal system: deep (>3 km deep) dilution between a southern high temperature upflow (~340 °C) and a conductively heated, low chloride fluid to the north (~290 °C); or two or more distinct upflows of differing chemistry and temperature in the south and north of the field (Winick et al., 2011). In either case, both models can be approximated in numerical models as several deep upflows with temperatures between 320-340 °C. Production chemistry data since the start of NAP has shown dilution and minor cooling in the northern part of the field (RK26, RK28 and RK13), confirming that a dilute, low chloride, fluid is being progressively drawn into the reservoir (Addison et al., 2015a). There are two possible

sources of this fluid; a deep, conductively heated fluid northwest of the current production wells and/or the overlying, lower chloride fluids within the intermediate aquifer and shallow aquifer. Some wells in the northwest of the field have also shown increasing chloride under production (RK17, RK27L2) that is most likely the result of boiling within the reservoir (Addison et al., 2015a).

2.2 Reservoir Extent

The interpreted extent of the permeable deep reservoir was derived from the combined interpretation of magnetotelluric (MT) and well data (natural state temperature and permeability) (Sewell et al., 2012). A transitional zone of lower permeability was defined by this approach that surrounds most of the permeable reservoir. Beyond the transitional zone is interpreted to be very low permeability, dominated by conductive heat transfer. A strong lateral gradient in natural state temperature occurs in the east between RK24 and RK19, suggesting a relatively sharp decrease in permeability occurs between the wells (Figure 3). RK24 has a convective, isothermal temperature profile with maximum measured temperature of 328 °C whilst RK19 has a conductive temperature profile, with maximum measured temperature of 200 °C, indicating it is outside the permeable geothermal reservoir. Natural state temperature in RK23 reaches a maximum of 300 °C, suggesting a similar transition in lateral temperature and permeability may occur in the southeast of the field. Both of these transitions in temperature are associated with a deeper clay cap imaged as low resistivity in MT surveys. The most uncertain areas of reservoir extent are in the south and the northwest. MT data around Lake Rotokawa show a deepening clay cap south of RK21/RK22, suggesting decreasing temperature and permeability, but this is unconfirmed by drilling. MT data northwest of the current production wells shows no deep clay cap, which is interpreted as being due to either unaltered volcanic formations or a previous higher temperature system similar to that imaged north of the Kawerau Field (Clark et al., 2015). Fluid inclusion and alteration in RK8 suggests higher temperatures existed in the past in the north than are currently measured (Rae et al., 2011). Further step-out drilling, particularly in the north and south of the field, may prove the current interpreted reservoir extent to be conservative.

2.3 Reservoir Permeability

The evolution of reservoir pressure since the start of NAP has been shown to be highly variable (Quiniao et al., 2013; Hernandez et al., 2015a). Strong lateral pressure gradients have developed in parts of the reservoir that appear to be controlled partly by geologic structures (Figure 4). Pressure drawdown is highest in the western part of the reservoir (~40 bar) and is elongated in a northeast-southwest direction. This is similar to the strike of the Production Field Fault and the strike of fractures identified in AFIT image logs in RK18L2 and RK32 (Figure 4). A tracer test conducted in 2006 showed first arrival of injection from RK18 to RK17 within a few days, with a tracer return profile characteristic of channelised flow (Addison et al., 2015b). It appears that production in this area is mostly along the strike of a major, generally high-permeability, structural zone associated with the Production Field Fault.

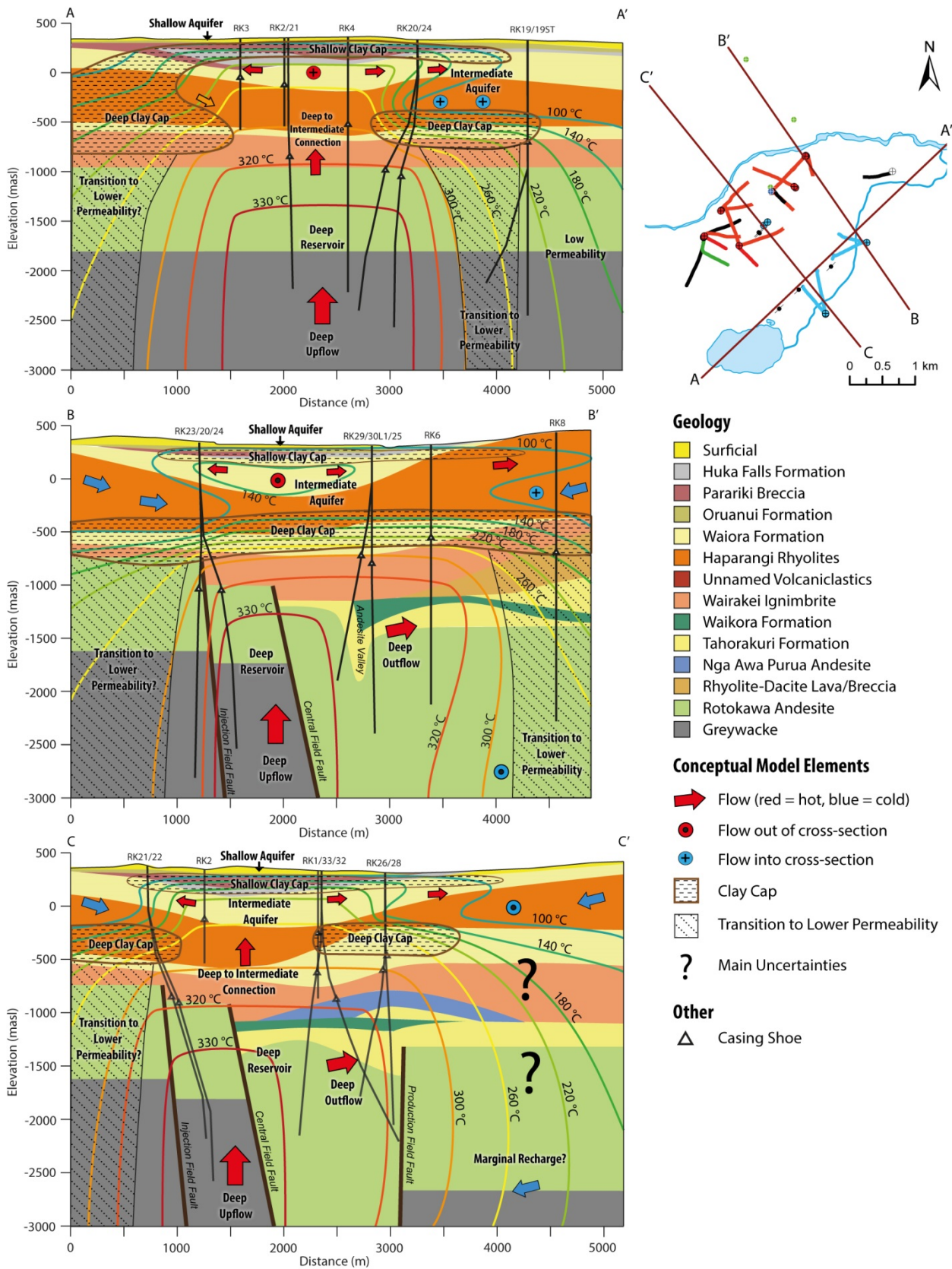


Figure 2: Conceptual model cross-sections (see inset and Figure 1 for location)

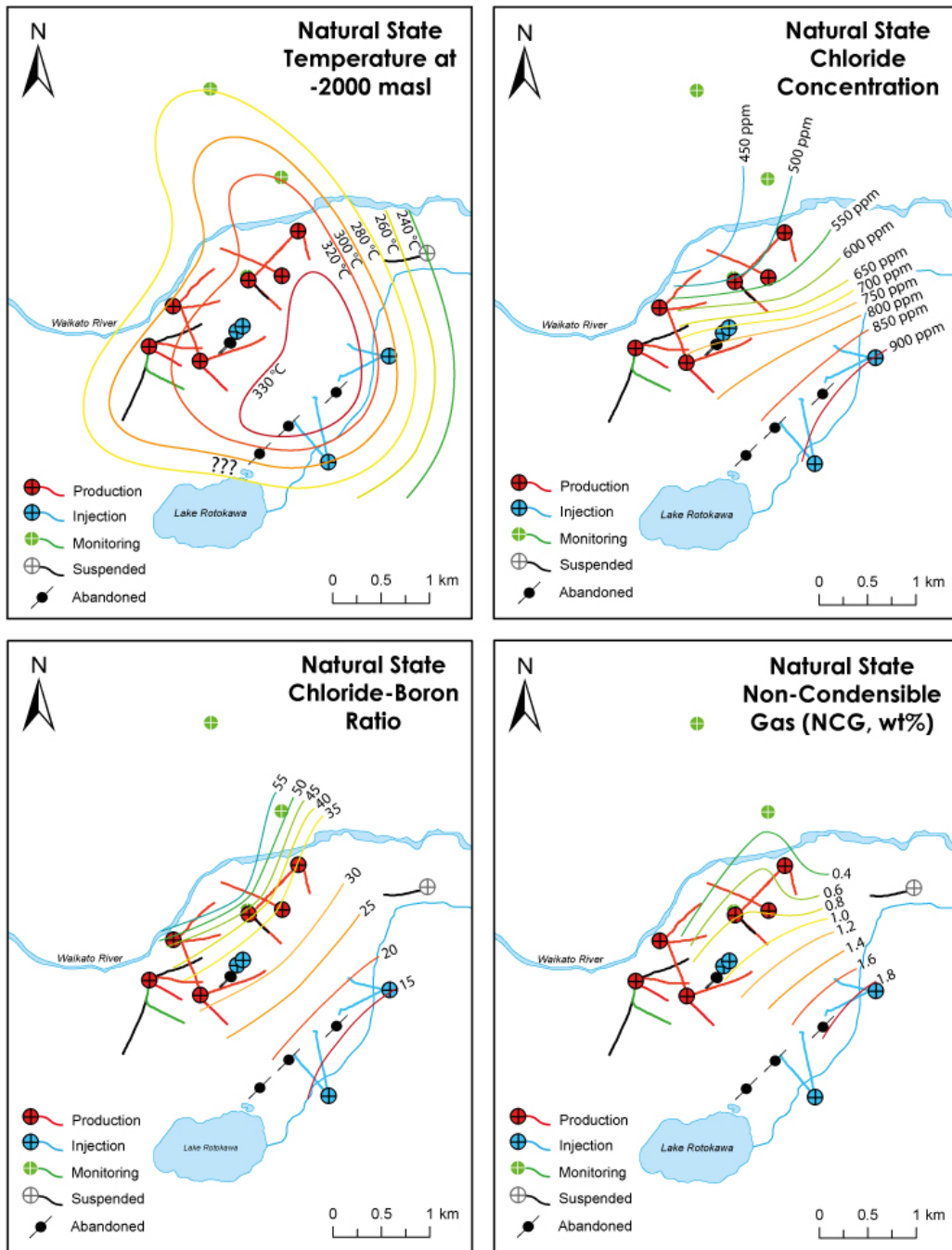


Figure 3: Natural state temperature and natural state chemistry of the deep reservoir. Both the temperature and chemistry indicate the main deep upflow to the geothermal system is in the southeast, with progressive cooling, dilution and gas loss towards the northwest. Natural state chemistry maps are modified after Winick et al., (2011).

A very strong lateral pressure gradient has developed between RK25/RK30 (~35 bar drawdown) and RK29 (~4 bar drawdown). This is despite RK29 being the highest producing well in the field, with average flow rates of 600-650 t/h. The gradient also appears to be oriented in a NE-SW structural direction, similar to the strike of fractures in the RK30L1 AFIT log, however there is currently no known structure identified through stratigraphic offset between RK29 and RK25/30. The gradient might be explained by the Andesite Valley in the RK30/25 area having limited connection to the wider andesite dominated reservoir. A gradient also appears to have developed between RK25/30 and RK6 (~3 bar drawdown). RK6 appears to have limited connection to the current production area, which might also be explained by the Andesite Valley in the RK30/25 area.

The Central Field Fault (CFF) also appears to be a major geologic structure that has a strong influence on fluid flow within the reservoir. A number of datasets strongly suggest the fault acts as a barrier to injection fluid flow across its strike (i.e., NW-SE direction), with enhanced permeability along strike. Recent tracer test results show injected fluid from RK24 first arrives at production wells after ~60 days, with ~12% of the injected fluid being returned to production wells (Addison et al., 2015b; Winick et al., 2015). The vast majority of microseismic activity since deep injection was moved to the south of the field has been on the injection side of a NE-SW trend that is interpreted to be the Central Field Fault (Figure 5). Together, the tracer results and the microseismicity strongly suggest the Central Field Fault acts to impede the flow of injection back to production. Other data suggests the CFF is permeable along

strike and up-dip. The projected surface trace of the CFF, as constrained by the microseismicity, appears to align a number of surface thermal features including Lake Rotokawa, several hydrothermal eruption craters and the Rotokawa Fumarole. Gas geothermometry (CO₂/Ar-H₂/Ar) of the Rotokawa Fumarole indicates that it is sourced directly from the deep (>300 °C) liquid reservoir with relatively minor intervening processes. The fumarole gas chemistry is also very similar in composition with gas obtained from a flow test of RK4 (N₂-He-Ar; Hedenquist et. al, 1988). This suggests the fumarole is sourced directly from the deep reservoir without significant residence time for re-equilibration in the overlying intermediate aquifer (Winick et al., 2011). The approximate surface trace of the fault also coincides with the area at the boiling point in its natural state from 100 to 1000 m depth, which extends in a relatively broad area from RK2-RK4 to RK1/11/12 (Sewell et al., 2012). These observations suggest that the fault likely acts as the main permeable connection between the deep reservoir and the intermediate aquifer, although there may be other permeable connections within the broader boiling-point-for-depth region.

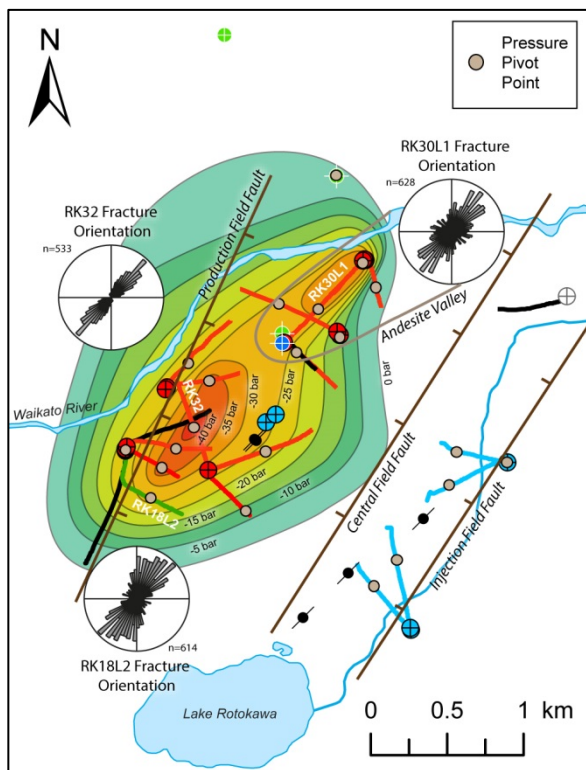


Figure 4: Comparison of reservoir pressure in 2015, with major geologic structures identified from stratigraphic offset (brown lines) and fracture orientation from AFIT image logs acquired in RK18L2, RK32 and RK30L1 (reservoir pressure contours from Hernandez et al., 2015a; fracture orientation data from McNamara et al., 2014).

2.4 Reservoir Base

The effective base of reservoir permeability for the numerical model was estimated to be between -3000 to -4000 masl based mostly on microseismic data. Microseismic activity at Rotokawa appears to be mostly related to injection cooling causing contraction of the reservoir rock that causes slip on pre-existing fractures

within the rock (Sewell et al., 2015). The majority of the microseismic activity at Rotokawa occurs at approximately the same depth as injection feedzones (-1500 masl to -3000 masl), and since the activity is mostly driven by cooling, this suggests that injected fluid does not sink much below the injection feed zones (Figure 5). This could be due to either the southern greywacke having poor vertical permeability or the injected fluid being quickly reheated to >300 °C preventing further sinking.

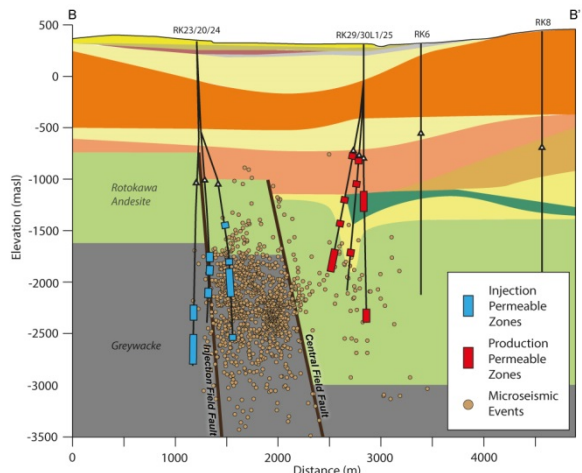


Figure 5: Microseismicity within 200 m of cross-section B-B' (see Figure 1 for location) from October 2008 to December 2012. The vast majority of the microseismicity occurs on the injection side of the Central Field Fault between -1500 to -3000 masl.

2.5 Reservoir Clay Cap

MT surveys, temperature profiles and clay type and content measurements (Methylene Blue, XRD and TerraSpec) show that the deep Rotokawa reservoir is capped in most places by a zone of low permeability, smectite/smectite-illite altered rock between approximately -400 to -750 masl (Figure 6). This is most often within the Waiaora Formation volcaniclastics and Wairakei Ignimbrite. Based on conductive natural state temperature profiles, the thickness of the cap varies significantly, from ~100-1000m.

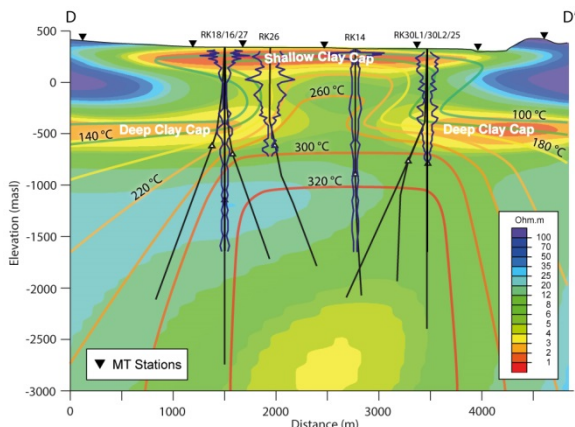


Figure 6: MT resistivity cross-section D-D' (see Figure 1 for location) with natural state temperature and smectite content (Methylene Blue, %) logs shown in blue along well tracks.

2.6 Connection between the Deep Reservoir and Intermediate Aquifer

In the natural state, the pressure differential between the deep reservoir and intermediate aquifer was approximately 10 bar. It follows that where there is significant permeability through the deep clay cap, an upflow of fluid from the reservoir into the overlying intermediate aquifer can occur. Where such an upflow occurs, natural state temperatures would be expected to be on or close to boiling-point-for-depth. Natural state boiling-point-for-depth temperature conditions occur at Rotokawa in a zone encompassing RK1, RK2, RK3, RK4 and RK11/12 (Figure 7). This matches well with a zone of higher resistivity (low conductance) imaged in MT surveys. The MT is imaging a zone of higher resistivity driven mainly by conversion of smectite and smectite-illite to higher order, less electrically conductive clays (e.g. illite and chlorite) due to temperatures being $>200^{\circ}\text{C}$. This is further supported by clay alteration mineralogy data (XRD, MeB and TerraSpec) obtained from the wells within the boiling-point-for-depth region. The main connection between the reservoir and intermediate aquifer is suspected to be along the Central Field Fault based on the gas geochemistry data from the Rotokawa Fumarole, which occurs along the surface trace of the fault, and the sharp lateral change in temperature within the intermediate aquifer between RK20/21/22/23/24 and RK2/3/4 (Figure 7).

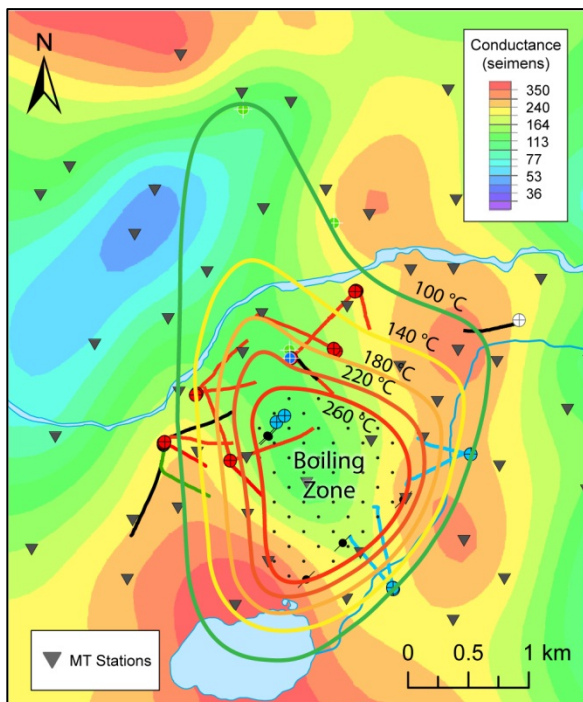


Figure 7: Deep MT conductance from 0 to -1000 masl (3D inversion) and isotherms of temperature at the bottom of the intermediate aquifer. An area of weakly developed clay cap in the south of the field (green-blue areas) coincides with boiling-point-for-depth conditions within the intermediate aquifer. Modified from Sewell et al., (2012).

2.7 Intermediate Aquifer

The intermediate aquifer is a laterally extensive, regional aquifer that contains variably mixed geothermal fluid and groundwater in the Rotokawa area. The aquifer is hosted within the Haparangi Rhyolite and Waiora Formation. Upflowing, boiling geothermal fluid flows into the intermediate aquifer through the zone of connection in the south (Figure 7). Cold, meteoric groundwater flows into the aquifer from topographically high areas, generally driving flow in the aquifer from south to north (Figure 7 & 8). The cooler flows largely occur within the Haparangi Rhyolites that outcrop in topographically high areas in the north and east (Figure 9).

Hot flows rise buoyantly to the base of the intermediate aquifer cap and flow to the north. Boiling, mainly within the connection area, releases gas (largely CO_2) that, when mixed with meteoric groundwater, forms slightly acidic (pH 5-6) bicarbonate fluids, which appear to be largely responsible for external casing corrosion issues at Rotokawa (Bowyer et al., 2008). Sulphate alteration, jarosite, anhydrite and alunite found in RK2, 3, 4, 14, 21, 22 between 100-500 mD indicates that sulphate fluid from the overlying shallow aquifer (see Section 2.9) may flow down into the intermediate aquifer through localized permeable paths in the overlying cap, particularly around Lake Rotokawa.

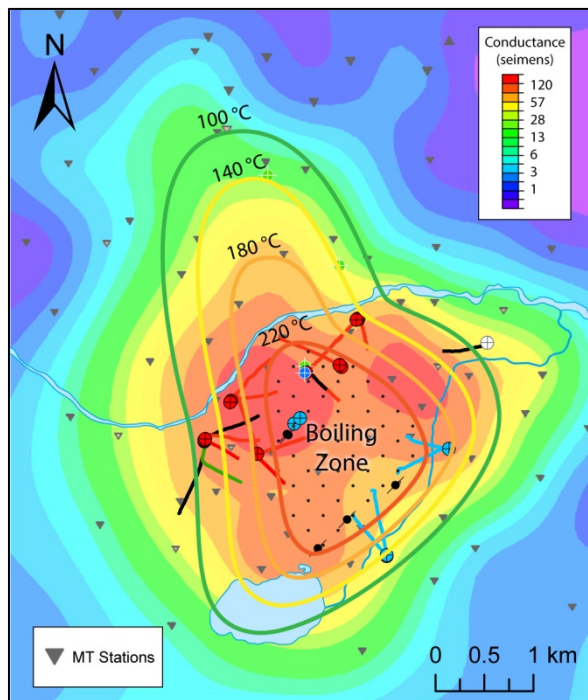


Figure 8: Shallow MT conductance from surface to 300 m depth (1D TE inversion) and isotherms of temperature at the top of the intermediate aquifer. The intermediate aquifer is capped by low resistivity (high conductance), smectite-altered formations. The area of shallow high conductance coincides well with the extent of the 100°C isotherm at the top of the aquifer. Modified from Sewell et al., (2012).

2.8 Intermediate Aquifer Clay Cap

Overlying the intermediate aquifer is another clay cap mostly within the Huka Falls Formation and Parariki Breccia. Smectite content within the cap is particularly high, lowering resistivity values to <2 ohm.m (Figure 6). Buoyant, hot flow at the top of the intermediate aquifer is pushed northward beneath the cap by groundwater flows. Steaming ground occurs in the north in the area where MT surveys show the shallow clay cap ends (Figure 8).

2.9 Shallow Aquifer

Overlying the intermediate aquifer cap is a shallow, unconfined aquifer from surface to approximately 100m depth. The aquifer is hosted mainly within the recent surficial deposits (Taupo Pumice Alluvium and Oruanui Formation). The aquifer drains into the Waikato River, the regional topographic low point. Geothermal input into the aquifer occurs from high chloride waters, thought to be sourced from the intermediate aquifer, that discharge into the surface aquifer mostly around Lake Rotokawa (Figure 9).

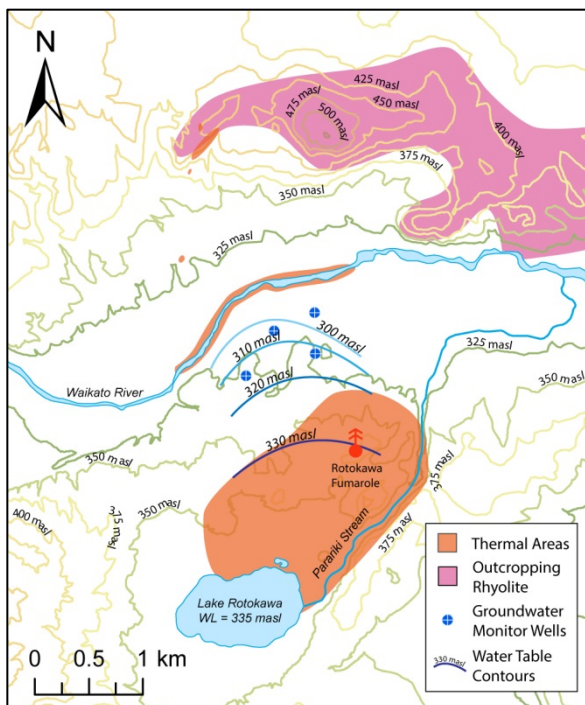


Figure 9: Shallow groundwater table contours (based on data from four shallow monitoring wells), thermal areas and outcropping rhyolites. Geothermal fluid discharged in thermal areas flows in the shallow aquifer under topographically driven pressure towards the Waikato River. Topography contours (25 m intervals) are also shown.

In this area, near-surface boiling releases H_2S gas that reacts with oxygen in the shallow groundwater and vadose zone to produce highly acidic ($pH < 2$) sulphate fluids. These are mixed with the high chloride and meteoric fluids that discharge from numerous hot springs into and around Lake Rotokawa and into the Parariki Stream. The Parariki Stream provides a direct drainage path from Lake Rotokawa into the Waikato River. Shallow groundwater wells, approximately 1 km down the hydraulic gradient from Lake

Rotokawa, discharge similar chloride-sulphate fluids consistent with shallow groundwater flow from the Lake Rotokawa area towards the Waikato River. Steam-heated, mixed bicarbonate and chloride fluids discharge at numerous hot springs along the banks of the Waikato River. On the northern side of the Waikato River, several areas of steaming ground occur in areas where the intermediate aquifer cap appears to end, suggesting these features are sourced from the intermediate aquifer. These generate similar sulphate and bicarbonate fluids in the shallow groundwater aquifer, which drain southwards into the Waikato River.

3. CONCLUSION

Collaboration between reservoir engineers, geochemists, geologists and geophysicists has produced a conceptual model consistent with most currently available datasets. Geochemistry and natural state temperatures show the main deep upflow to the system is likely in the south, with deep outflow towards the north. The reservoir is capped in most places by a layer of smectite/smectite-illite altered rock. Overlying this cap is an intermediate aquifer of mixed geothermal and meteoric fluids hosted mostly within rhyolite lavas and volcaniclastic sediments. A zone of higher permeability through the reservoir cap in the south of the field allows fluid to flow from the reservoir into the overlying intermediate aquifer, creating boiling-point-for-depth temperature conditions. The main permeable connection between the reservoir and intermediate aquifer is considered to be along the Central Field Fault. Boiling fluid rises buoyantly to the top of the intermediate aquifer and is pushed mainly northwards by cooler, meteoric fluid flow from the south. Meteoric flows within the aquifer are driven by higher topography, including outcropping rhyolite domes, surrounding the field. The intermediate aquifer is capped in the Rotokawa area by a layer of high smectite clay, mostly within the lacustrine sediments of the Huka Falls Formation and Parariki Breccia. Localised permeability through this cap allows fluid flow through to the overlying surface features and surface aquifer. Mixed sulphate-chloride-bicarbonate waters occur within this aquifer that ultimately drain into the Waikato River.

The main change to the conceptual understanding of the field since the start of the NAP plant has been that permeability within the reservoir appears to be highly variable as seen from the highly varied reservoir pressure evolution over time. It appears this is at least partly controlled by geologic structure. Continued operation of the field and future drilling will increase understanding of the permeability variations.

Further work on the existing wells, continued collection of reservoir monitoring data and further drilling will lead to continued refinement of the conceptual model.

ACKNOWLEDGEMENTS

The authors wish to sincerely thank the Rotokawa Joint Venture (Mighty River Power and Tauhara North No.2 Trust) for permission to publish this paper.

MRP Geoscience staff that have contributed to the development of the conceptual model since NAP start include; Candice Bardsley, Irene Wallis, Jaime Quinao, Jonathon Clearwater, Farrell Siega, Etienne Buscarlet. Ex-

MRP Geoscience staff that have contributed include; Jeff Winick, Jeremy O'Brien, Linda Price, Deborah Bowyer.

Tom Powell and Bill Cumming also contributed extensively to the development of the Rotokawa conceptual model presented here.

GNS Science contributed significantly to the conceptual model by providing well site geology and alteration, microseismic data, AFIT log interpretation and geochemistry analysis.

REFERENCES

- Addison, S., Winick, J., Sewell, S., Buscarlet, E., Siega, F., Hernandez, D., (2015a). Geochemical response of the Rotokawa reservoir to the first five years of Nga Awa Purua production. Proceedings of 38th New Zealand Geothermal Workshop 2015, Taupo.
- Addison, S., Winick, J., Mountain, B., Siega, F., (2015b) Rotokawa reservoir tracer test history. Proceedings of 38th New Zealand Geothermal Workshop 2015, Taupo.
- Bowyer, D., Bignall, G., Hunt, T., (2008). Formation and neutralization of corrosive fluids in the shallow injection aquifer, Rotokawa Geothermal Field, New Zealand. Geothermal Resources Council Transactions. 32.
- Bowyer, D., Holt, R., (2010). Case Study: Development of a numerical model by a multi-disciplinary approach, Rotokawa Geothermal Field, New Zealand. Proceedings World Geothermal Congress 2010, Bali, Indonesia.
- Browne, P. R. L., (1989). Investigations at the Rotokawa Geothermal Field, Taupo Volcanic Zone, New Zealand. Journal of Geothermal Research Society of Japan. 11 (2), p87-96.
- Clark, J., Milicich, S., Sewell, S., Askari, M., Wong, C., (2015). Finding sufficient permeability for outfield injection and recent drilling at Kawerau, New Zealand. Proceedings World Geothermal Congress 2015, Melbourne, Australia.
- Grant, M. (1985). Pressure and permeability distribution in Rotokawa Geothermal Field. DSIR Report No. 123
- Grindley, G. W., Browne, P. R. L., Gardner, M., (1985). Surface and subsurface geology, Rotokawa Geothermal Field. Ministry of Works and Development Report to the Ministry of Energy, New Zealand.
- Hedenquist, J., Mroczek, E., Giggenbach, W., (1988). Geochemistry of the Rotokawa Geothermal system: Summary of data, interpretation and appraisal for energy development. Chemistry Division DSIR Technical Note. 88 (6).
- Hernandez, D., Addison, S., Sewell, S., Azwar, L., Barnes, M., (2015a). Rotokawa reservoir response to 172 MW of geothermal operation. Proceedings of 38th New Zealand Geothermal Workshop 2015, Taupo.
- Hernandez, D., Clearwater, J., Burnell, J., Franz, P., Azwar, L., Marsh, A., (2015b). Update on the modeling of the Rotokawa Geothermal System: 2010 – 2014. Proceedings World Geothermal Congress 2015, Melbourne, Australia.
- McNamara, D., Massiot, C., Lewis, B., Wallis, I., (2014). Heterogeneity of structure and stress in the Rotokawa Geothermal Field, New Zealand. Journal of Geophysical Research Solid Earth. 120. p1243-1262.
- McNamara, D., Sewell, S., Buscarlet, E., Wallis, I., (2015). A review of the Rotokawa Geothermal Field, New Zealand. Geothermics. In Press.
- Quinao, J., Azwar, L., Clearwater, J., Hoepfinger, V., Le Brun, M., Bardsley, C., (2013). Analysis and modeling of reservoir pressure changes to interpret the Rotokawa Geothermal Field response to Nga Awa Purua Power Station operation. Proceedings Thirty-Eighth Workshop on Geothermal Reservoir Engineering. Stanford University, Stanford, California.
- Sewell, S. M., Cumming, W., Bardsley, C., Winick, J., Quinao, J., Wallis, I., Sherburn, S., Bourguignon, S., Bannister, S., (2015). Interpretation of microseismicity at the Rotokawa Geothermal Field, 2008 to 2012. Proceedings World Geothermal Congress 2015, Melbourne, Australia.
- Sewell, S. M., Cumming, W. B., Sirad-Azwar, L., Bardsley, C. (2012). Integrated MT and natural state temperature interpretation for a conceptual model supporting reservoir numerical modeling and well targeting at the Rotokawa Geothermal Field, New Zealand. Proceedings Thirty-Seventh Workshop on Geothermal Reservoir Engineering. Stanford University, California.
- Rae, A., O'Brien, J., Ramirez, E., Bignall, G., (2011). The application of chlorite geothermometry to hydrothermally altered Rotokawa Andesite, Rotokawa Geothermal Field. Proceedings New Zealand Geothermal Workshop 2011, Auckland, New Zealand.
- Winick, J., Powell, T., Mroczek, E. (2011). The natural-state geochemistry of the Rotokawa reservoir. Proceedings New Zealand Geothermal Workshop 2011, Auckland, New Zealand.
- Winick, J., Siega, F., Addison, S., Richardson, I., Mountain, B., Barry, B., (2015). Coupled Iodine-125 and 2NSA reservoir tracer testing at the Rotokawa Geothermal Field, New Zealand. Proceedings World Geothermal Congress 2015, Melbourne, Australia.